Original Research Article

J. Funct. Mater. Biomol. 2(2)-2018 pp 40-47

SACRED HEART RESEARCH PUBLICATIONS

Journal of Functional Materials and Biomolecules

Journal homepage: www.shcpub.edu.in

ISSN: 2456-9429

Synthesis of colloidal copper nanoparticles and their ability to modify the DNA structure in a programmable pathway

***NatarajanPrabakaran* [*1,2], *Sepperumal Murugesan*[1], *and Periakaruppan Athappan*[1]**

Received on 14 Oct 2018, Accepted on 10 Nov 2018

Abstract

Synthesis of tetrapodal structured cationic cetyltrimethylammonium bromide stabilized copper nanoparticles (CTAB-CuNPs) and spherical shaped anionic sodium dodecyl sulphate stabilized copper nanoparticles (SDS-CuNPs), which are stable for more than 100 days in aqueous solutions, by chemical reduction under sonication is reported. The differences in their binding with DNA and the changes in the structural morphology on a programmable way were studied through UV-vis spectroscopic, atomic force microscopic (AFM), scanning electron microscopic (SEM), transmission electron microscopic (TEM), emission and electrophoresis techniques. The circular dichroic (CD) spectral studies reveal the significant effect of CTAB-CuNPs in transforming B to Z conformation in CT-DNA. At lower concentrations, copper nanoparticles form spaghetti/ellipsoid like structures with DNA, while at higher concentrations cleaves the DNA and form discrete chain-like assemblies. The emission and gel electrophoresis studies also support these findings.

Keywords: Copper nanoparticles; nanoparticle-DNA interaction; tetrapodal assembly; groove binding; CD spectroscopy.

1 Introduction

Inorganic nanostructures have attracted much attention due to recent exploitation of novel size dependent chemical and physical properties as well as potential applications as nano devices. A burst of research activity is witnessed in recent years in the area of synthesis and fabrication of metal and semiconductor nanoparticles, having different size and shape, because of their novel optical, catalytic, electrical and magnetic properties and their applications in designing advanced materials as nanoscale building blocks [1-6]. In particular, size and shape controlled composite nanoparticles with well-defined structures favour many applications. Now-a-days, though many methods including ball milling [7], pulsed electro deposition [8], reduction of metal salts [9], reverse micelle process [10], vapor deposition [11] and hydrothermal-reduction [12] are developed for preparation of nano sized metal particles, chemical reduction is the most convenient method for synthesis of metallic nanoparticles, since it yields a large variety of dispersions in terms of their particle size, morphology and stability [4-6]. Copper nanoparticles (CuNPs) are prepared mostly in aqueous solutions containing polymers or surfactants as stabilizer, which inhibit the oxidation of Cu atoms. Huang et al. prepared copper nanoparticles in aqueous solutions of polyvinylpyrrolidone by chemical reduction method [13]. Wu and Chen synthesized copper nanoparticles with Cu concentration as high as 0.2 M using the surfactant cetyltrimethylammonium bromide (CTAB) as stabilizer [14]. Zhang et al. reported the preparation of copper nanoparticles using Tweens and/or sodium dodecyl sulfate (SDS) and showed that the particle size was dependent on the nature of surfactant [15]. Lisiecki et al. suggested that the SDS play an important role on the shape and size of copper nanoparticles [16]. Khanna et al. prepared copper nanoparticles with the use of $CuCl_2$, hydrazine and polyvinyl alcohol and found that addition of carboxylic acids or their salts such as trisodium citrate and myristic acid are more effective in inhibiting the oxidation of Cu nanoparticles [17]. The main difficulty in the use of copper nanoparticles in aqueous medium arises due to their instability as they are oxidized by the dissolved air. Therefore, it is required to develop methods to improve the chemical stability of Cu nanoparticles in hydrophilic medium for application oriented practical reasons.

Among the different kinds of methodologies developed for one-dimensional organization, the linear self-assembly of gold nanoparticles carrying polynucleotide chains [18] and the electrostatic interaction of cation-charged nanoparticles on the anion-charged DNA [19,20] are found to be promising. Interestingly, the DNA directed fabrication of metallic copper nanostructures has remained elusive. Monson et al. reported the surface-attached metallization of DNA with copper to create nanowires up to 6 nm tall [21]. The delivery of a drug at the site of action, to avoid the side effects, is a major concern because it has to cross many barriers and

* Corresponding author: e-mail an.prabakar@gmail.com, Phone: +0452-268032.
[1] School of Chemistry, Madurai Kamaraj University, Madurai-21
[2] Assistant Professor, Department of Chemistry, Yadava college, Madurai-14: 9787147490: 0452-2697093.

boundaries before being delivered at the site. The fine tuning of nanoparticles will enable them to be used as carriers of drugs that will lead to a targeted delivery system suitable for clinical use [22]. In our laboratory, non-covalent DNA binding of transition metal complexes, especially copper [23], and self-assembly of nickel nanoparticles on DNA have been extensively studied [24]. In this paper, we report the synthesis and characterization of highly stable colloidal CuNPs in aqueous medium and their effect of concentration on DNA to form chain like and ellipsoid structures which may pave way to design a powerful drug delivery system. The interaction between CuNPs and DNA has been investigated using host of methods like UV-vis, emission and CD spectral studies, gel electrophoresis and viscosity measurements. The SEM, TEM and AFM techniques were also used to corroborate the findings.

2 Experimental

2.1. Reagents and Materials

Copper chloride dihydrate ($CuCl_2 \cdot 2H_2O$; Merck) was used as copper precursor. Cetyltrimethylammonium bromide (CTAB; Merck), sodium dodecyl sulfate (SDS; Merck) and citric acid monohydrate (Sigma-Aldrich) were used as stabilizers. Hydrazine monohydrate (Merck) was used as a reducing reagent. Tetraethylorthosilane (TEOS; Aldrich, 97%) was used for silica-coating and ammonia solution (Merck) was used for adjusting the pH. All chemicals were of analytical grade and were used as received. Herring sperm DNA (Sisco research laboratory, India), Calf-thymus DNA (CT-DNA) and pUC18 DNA (GeNei, India) were used for the CuNPs-DNA binding studies. Tris-base, bromophenol blue, xylene cyanol, glycerol, acetic acid, sodium hydroxide and ethylenediaminetetraacetic acid (EDTA; Merck) were used for TEA buffer preparation. Ultrapure double distilled water was used in all the preparations and was deaerated by bubbling with N_2 gas for 30 min prior to the preparation of aqueous solutions of $CuCl_2$ and hydrazine.

2.2. Synthesis of copper nanoparticles

Colloids of copper nanoparticles in cetyltrimethylammonium bromide (CTAB-CuNPs) and in sodium dodecyl sulfate (SDS-CuNPs) were prepared through a modified procedure [25]. Accordingly, 10 mL of freshly prepared 0.2 M aqueous hydrazine solution containing 0.005 M CTAB or SDS and 0.0005 M citric acid was added to 10 mL of 0.002 M $CuCl_2$ aqueous solution containing 3 mL of the 0.005 M CTAB or SDS and 5 mL of 0.001 M citric acid under sonication. Colour of the mixture turned reddish brown gradually in 30 min duration due the formation of copper nanoparticles and this colloidal solution was used for further studies.

2.3. Silica-coating

The SDS-CuNPs (0.3 mL) were made up to 10 mL with deaerated double distilled water and 1 mL of TEOS in H_2O was added drop-wise under sonication, and the sonication was continued for about 30 min. To this, 2 mL of 25% liquid NH_3 was added drop-wise under sonication and the sonication was continued for 1 h. During this period, the brown-red colloidal solution changed to bluish white. This colloidal solution was filtered through Whatmann No 1 filter paper and the filtrate was used for further characterization.

2.4. Characterization

The CTAB-CuNPs, SDS-CuNPs and silica-coated SDS-CuNPs were characterized by UV-vis spectroscopy, scanning electron microscopy (SEM), transmission electron microscopy (TEM) and atomic force microscopy (AFM). UV-vis extinction spectra were measured with a Jasco J-550 spectrophotometer. SEM images were recorded using a Hitachi S-3400 scanning electron microscope operating at 20 kV. TEM images were performed with a JEOL 3011 transmission electron microscope operating at 200 kV. Samples for TEM were prepared by dropping and evaporating the nanoparticle suspensions on a copper grid under nitrogen atmosphere. Samples for SEM and AFM were prepared by dropping and evaporating the nanoparticle colloids on a glass plate. AFM analysis was performed using AFM A100 SGS scanning probe microscope. The interactions of these nanoparticles with Calf-Thymus DNA were studied through circular dichroism (CD) spectra using a Jasco J-810 spectropolarimeter. The emission spectral studies were made using a Jasco FP-6300 spectrophotometer. To explore the binding further, viscosity measurements were performed at 27 ^{o}C with a BROOKFIELD, DV-II+ Pro viscometer.

2.5. pUC18 DNA Cleavage

pUC18 DNA (8 µL, 150 µg) were placed in 0.5 mL polymerized chain reaction (PCR) tube and 5 to 20 µL of colloidal CuNPs (20-160 µM range) were added and the mixtures were allowed to stand at 37 ºC for 90 min, after which 5 µL of a loading buffer solution (0.25% Bromophenol blue, 0.25% Xylene cyanole, and 30% glycerol) was added. The solution underwent electrophoresis on a 0.8% agrose gel in 0.5X TAE buffer [10 mL of 0.5 M EDTA (18.63 g EDTA dissolved in 80 mL of distilled water and the pH was adjusted to 8.0 using 1N NaOH and the final volume was made up to 100 mL), and 2.42 g Tris base in 50 mL of distilled water were added with 5.71 mL of glacial acetic acid mixed well and made up to 100 mL with distilled water] containing 15 µL/100 mL of EB solution at 60 mV applied voltage for about 90 min. Electrophoresis experiments were carried out using a LARK- DYY-6C power supply unit with GeNei UV-illuminator. The gel was photographed using a BIORAD system.

3 Results and Discussion

3.1. UV-visible spectroscopy

The absorption spectra of cationic, CTAB-CuNPs and anionic, SDS-CuNPs colloids exhibit (Figure 1) surface plasmon resonance (SPR) peaks at 589 and 594 nm respectively, attributable to the presence of copper

nanoparticles [16-17]. The difference in the surface plasmon resonance peaks indicates that the SDS-CuNPs clusters are slightly bigger in size than those of CTAB-CuNPs clusters. The intensity of SPR peak for CTAB-CuNPs clusters was not affected even after 100 days and then slowly decreases with broadening. Interestingly, for the SDS-CuNPs clusters, the SPR peak intensity is found to be not affected even after 20 weeks. These results indicate that the CuNPs were chemically stable in aqueous solution at least for 100 days and the extra stability acquired by the CuNPs prepared in SDS may be due to the presence of negative dipole in the SDS, which is expected to repel and inhibit the entry of negative dipole oxygen atoms into the clusters.

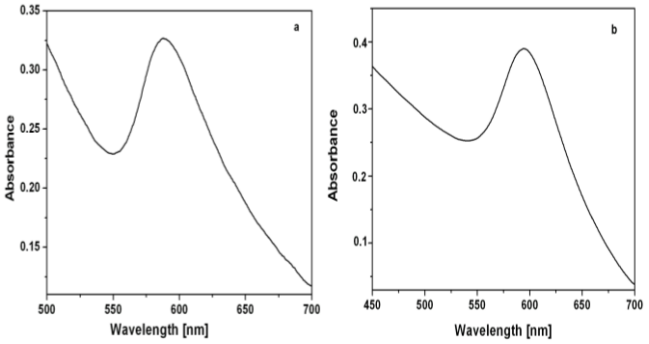

Figure 1. Electronic spectra of CuNPs in (a) citric acid with CTAB and (b) citric acid with SDS

3.2. SEM, TEM and AFM studies

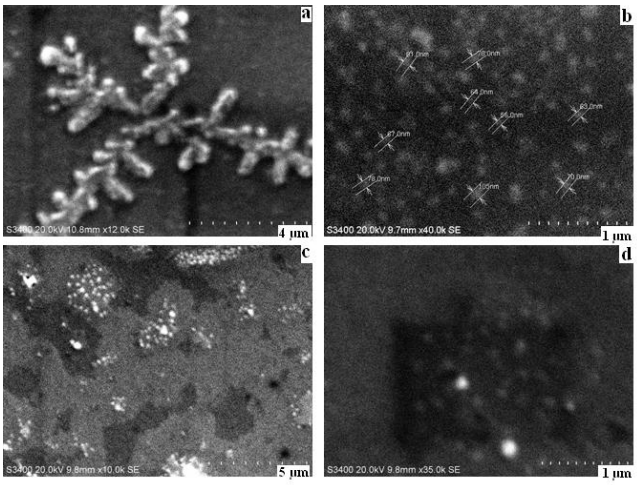

Figure 2. SEM images of CuNPs in CTAB (a & b) and in SDS (c & d)

SEM images of the CTAB-CuNPs and SDS-CuNPs in aqueous dispersion are given in figure 2. CTAB-CuNPs exhibit neatly assembled dendrimers with tetrapodal structures. The magnified image of tetrapodal arrangement (Figure 2b) reveals that they contain copper nanoparticle agglomerates of 60–70 nm size. Whereas, SDS-CuNPs do not form dendrimers and the size of the spherical agglomerates is about 100 nm in size (figure 2c and 2d). Due to the extra stability of SDS-CuNPs, which is present in the SO_4^- ion in the shell. we decided to extend our interest in them and functionalize these CuNPs using TEOS. The SEM image (figure 3) of TEOS functionalized SDS-CuNPs shows that the morphology of the CuNPs were not changed during functionalization but the size of the grains increased due to coverage of the nanoparticle surface by silicate network.

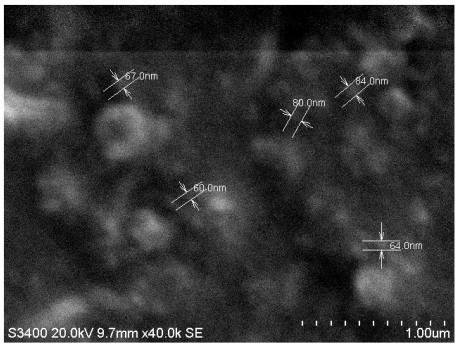

Figure 3. SEM image of SDS capped CuNPs functionalized with TEOS

The TEM image of CTAB-CuNPs (Figure 4) shows that the clusters observed in SEM are composed of copper nano particles of about 10 nm in size, while SDS-CuNPs are little bit bigger and are about 15 ± 2 nm in size. The morphology of CuNPs in TEM images is in agreement with the SEM results and the SDS-CuNPs functionalized with TEOS have particles of 20–30 nm in size (Figure 5). The long stable Cu colloidal solutions when exposed to atmospheric air, the SDS-CuNPs colloid loses its colour slowly in 15 days, where as CTAB-CuNPs colloids in 4 days and the dendrimer structure was found to be disturbed (Figure 6). This suggests that the CuNPs leached out of capping agents and get oxidized. The AFM results also confirm the above findings and are given in supporting information (Figure S1 in the supporting information).

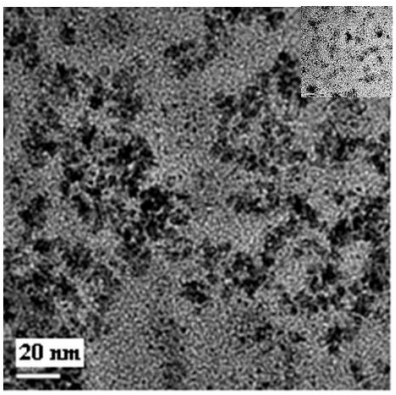

Figure 4. TEM image of CTAB stabilized CuNPs

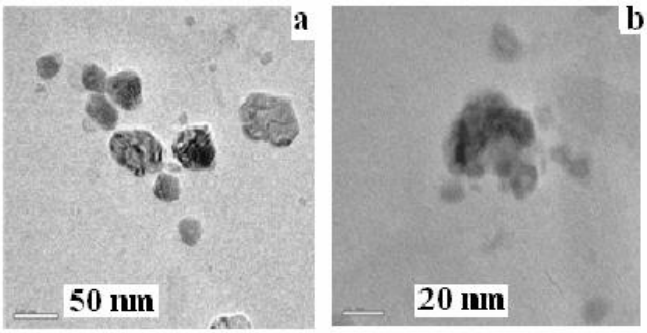

Figure 5. TEM image of TEOS functionalized CuNPs

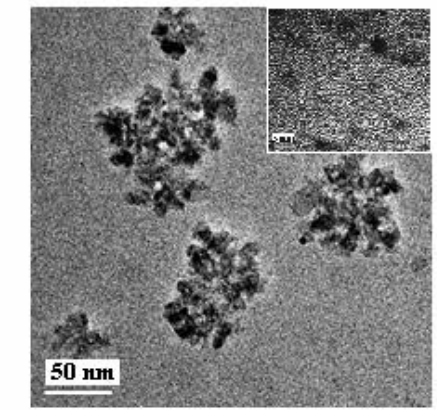

Figure 6. TEM image of CuNPs, after 7 days keep in atmospheric air. (Insert: its HRTEM image)

3.3. DNA binding study

3.3. 1. UV-vis absorption spectra

In order to investigate the interaction of DNA with the synthesized copper nanoparticles, the CTAB-CuNPs and SDS-CuNPs colloids were diluted with deaerated water and the corresponding SPR peaks were found to be shifted to 592 nm from 589 nm and to 589 nm from 594 nm respectively. This shift may be attributed to the redistribution of colloids with uniform size due to the surface interaction of the surrounding medium. When the CTAB-CuNPs were titrated with herring sperm DNA ((λ_{max} = 260 nm, ε = 6600 $mol^{-1}\,dm^3\,cm^{-1}$; 100 μM solution) the peak at 591 nm undergo 23.96% hypochromism along with 5 nm red shift, while for the SDS-CuNPs 9.88% hypochromism and 3 nm red shift were observed at 589 nm. The percentage of hypochromism observed in the visible region for the cationic CTAB capped CuNPs is much higher than for the anionic SDS capped CuNPs and the observed hypochromism for the initial addition of DNA is higher than those of subsequent additions and attains saturation at higher concentrations of DNA (3.02 μM) and are given in Table 1.

To evaluate the differences in the hypochromism and in the red shift, the binding strengths of CTAB-CuNPs and SDS-CuNPs quantitatively with herring sperm DNA, their intrinsic binding constants were obtained by monitoring the changes in the absorbance at 591 and 589 nm (Figure 7), respectively, during the addition of increasing concentrations of DNA using the following equation [23,26].

$$[DNA]/(\varepsilon_a - \varepsilon_f) = [DNA]/(\varepsilon_b - \varepsilon_f) + 1/[K_b(\varepsilon_b - \varepsilon_f)] \quad \ldots\ldots\ldots\ldots (1)$$

where ε_a, ε_f and ε_b respectively correspond to the observed extinction coefficient for each addition of DNA to CuNPs, the extinction coefficient for the free CuNPs and the extinction coefficient for the CuNPs in the fully bound form. Plot of $[DNA]/(\varepsilon_a - \varepsilon_f)$ *versus* [DNA] gave a slope of $1/(\varepsilon_b - \varepsilon_f)$ and the intercept equal to $1/[K_b(\varepsilon_b - \varepsilon_f)]$; K_b was obtained from the ratio of the slope to the intercept. The evaluated intrinsic binding constants (K_b) respectively for CTAB-CuNPs and SDS-CuNPs were found to be 1.089×10^5 M^{-1} and $9.8 \times 10^4\,M^{-1}$. We expected a vast difference in their binding constants as the cationic CuNPs may easily be attracted by the negatively charged DNA when compared to anionic CuNPs, where repulsion is expected. The small difference in their binding constants may be ascribed to the time delay in masking the free discrete CuNP clusters by the more and more DNA polymeric units, while they are released from the capping agents through the rupture by the molecules in the surrounding medium.

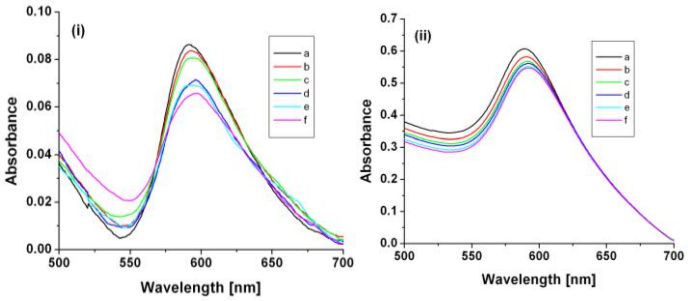

Figure 7. Electronic spectra of CuNPs capped with (i) CTAB and (ii) SDS in 50 mM Tris-HCl and 50 mM NaCl buffer, pH 7.13, in the presence of increasing amounts of DNA (a-f corresponds to 0–5.2 μM)

However, when increasing amounts of CTAB-CuNPs are titrated with a fixed concentration of DNA, hyperchromism occurs up to a particular concentration and then it becomes hypochromic (Figure S2a in the supporting information). The hyperchromism at low concentration of CuNPs may be due to their binding in the minor grooves of the DNA [27], and at higher concentrations of CuNPs the excess Cu nanoparticles bind in the major grooves and hence it becomes hypochromic [28], that is expected to invert the B conformation in to the Z conformation (vide infra CD spectra). While for SDS-CuNPs, with increasing amounts of CuNPs only hyperchromism (Figure S2b in the supporting information) is observed due to the repulsive interaction of anionic SDS and anionic DNA polymers. The delay in the interaction may be due to the need for the interposition of water molecules in between the repulsive DNA and SDS molecules that would make H-bond and cleave the SDS to release the CuNPs.

Table 1. Electronic spectral data of CuNPs on titration with DNA and vice-versa

Colloidal solution	λ_{max} nm				Binding constant (K_b)
	Free	Bound	$\Delta\lambda_{max}$ nm	%Ha	
CTAB-CuNPs vs. DNA	591	596	5	23.96	1.09×10^5 M^{-1}
SDS-CuNPs vs. DNA	589	592	3	9.88	9.81×10^4 M^{-1}
DNA vs. CTAB-CuNPs	260	262	2	7	1.13×10^5 M^{-1}
DNA vs. SDS-CuNPs	260	262	2	5	4.21×10^3 M^{-1}

a % H $= 100(A_{free} - A_{bound})/A_{free}$

The above results reveal that the cationic CTAB-CuNPs bind with DNA in a better way than the anionic SDS-CuNPs and invert B to Z conformation. The binding constant of the anionic SDS-CuNPs with DNA seems to be dependent on the slowly released CuNPs from the negatively charged capping agent, SDS.

3.3. 2. Competitive binding

As the CuNPs are non-emissive, competitive binding studies with ethidium bromide (EB) were carried out to gain support for the mode of binding of the CuNPs with DNA. EB does not show any emission in Tris-HCl buffer due to fluorescence quenching of the free EB by the solvent molecules [29]. The study involves the measurement of emission intensity for each addition of CuNPs to herring sperm DNA, pretreated with EB. A fixed concentration of 50 µM EB solution and 42 µM of herring sperm DNA were placed in a 5 mL test tube. The mixture of DNA-EB was titrated with increasing amounts of CuNPs, where a considerable drop in the emission intensity (Figure S3 in the supporting information) was observed.

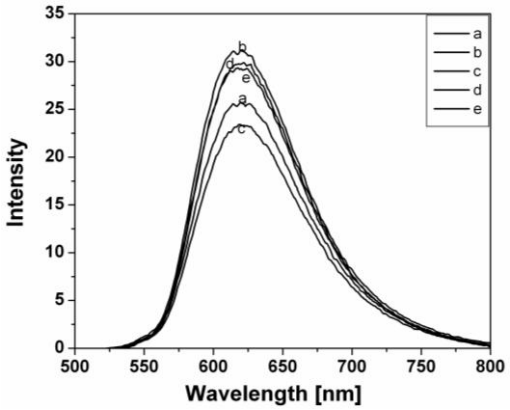

Figure 8. Emission spectra of (a) EB, (b) EB+DNA, (c) b+23 µM CTAB-CuNPs, (d) b+23 µM SDS-CuNPs and (e) b+23 µM TEOS-CuNPs

The quenching of EB-DNA followed the Stern-Volmer relationship of the form:

$$F_o/F = 1 + K_{sv}[Q] \quad \ldots\ldots\ldots\ldots \quad (2)$$

Where, F_o and F are the fluorescence intensities of the excited EB-DNA respectively in the absence and presence of CuNPs, the quencher concentration [Q] and $K_{sv,}$ the Stern-Volmer constant. The plots of F_o/F *vs* CuNPs concentration [Q] evolved quadratically and are found to be affected by [Q]. The binding constant values (K_{sv}) calculated from the above equations are 3.71×10^4 M^{-1} for CTAB-CuNPs, 1.71×10^4 M^{-1} for SDS-CuNPs and 2.41×10^4 M^{-1} for TEOS-CuNPs. Figure 8 shows that the colloidal CuNPs encapsulated in CTAB binds much better than the TEOS and SDS stabilized CuNPs. Also the fluorescence quenching observed while CTAB-CuNPs was added is much higher than the others. The extraordinary behavior of CTAB-CuNPs in fluorescence quenching may be due to the conformational changes in the DNA structure (vide infra CD spectra).

3.3. 3. Viscosity measurement

To further clarify the nature of the interaction between the CuNPs and herring sperm DNA, viscosity measurements were carried out and the results are presented in Figure S4 in the supporting information. Intercalation is expected to lengthen the DNA helix as the base pairs are pushed apart to accommodate the bound molecule, leading to increase in the DNA viscosity. A classical intercalator such as ethidium bromide (EB) could cause a significant increase in viscosity of DNA solution. In contrast, partial non-classical intercalators, binding through the grooves, could bend (or kink) the DNA helix, reduce its effective length and concomitantly its viscosity [30,31]. Increasing concentration of CuNPs initially increases the viscosity for one or two additions and for subsequent additions the viscosity gradually decreases and reaches saturation (Figure S4 in the supporting information). This behaviour could be explained on the basis of slow incorporation of CuNPs in the DNA grooves which could kink the DNA helix.

3.3. 4. Circular dichroism spectra

CD spectroscopic technique is useful in monitoring the conformational variation of DNA in solution, as the band due to base stacking (278 nm) and that due to right handed helicity (244 nm) are quite sensitive to the mode of DNA interactions with small molecules [32]. The CD spectra of the DNA with increasing concentrations of CTAB-CuNPs in the 9.3 µM to 70 µM (Figure 9) show that with 9 µM of CTAB-CuNPs the DNA undergoes chiral inversion of the spectra, which on increasing the concentration both positive and negative bands are blue shifted. This reveals that the presence of highly charged cationic CTAB-CuNPs in the minor and major grooves facilitates the transformation of the DNA from B to Z conformation [33-35], and at still higher concentrations, they kink and cleave the DNA completely in to the constituent nucleotides. On the other hand, during the addition of increasing concentrations of SDS stabilized CuNPs (Figure S5i. in the supporting information), the positive band intensity increases with a slight red shift, while the negative band intensity increases a little bit

without any remarkable red shift. For the TEOS topped SDS-CuNPs the increasing amounts of CuNPs (Figure S5ii. in the supporting information) also increase the intensity of both positive and negative bands without any shift in their position. These results show that there is no conformational change in base stacking but only the helicity is affected due to the incorporation of nanoparticles in the grooves.

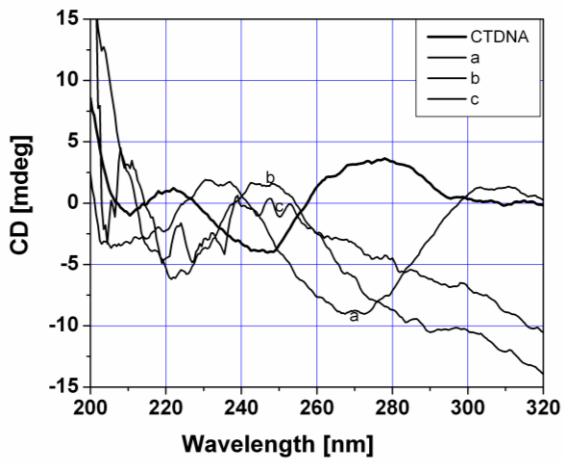

Figure 9. CD spectra of CT-DNA in the presence of increasing amounts of CTAB capped CuNPs in 50 mM Tris-HCl and 50 mM NaCl buffer, pH 7.13; [a = 9.3μM, b = 23 μM and c = 70 μM CuNPs]

3.3. 5. pUC18 DNA cleavage

In order to identify whether cleavage occurs or not, gel electrophoresis experiments were carried out at pH 8.1 using TEA buffer with varying concentration CuNPs stabilized in CTAB, SDS and TEOS on pUC18 DNA (Figure 10). Lane C represents pUC18 DNA control. Lane 1-5 represents the effect of CTAB-CuNPs with increasing concentration of CuNPs (5, 7, 10, 12.5, and 16.5 μM), where the DNA band disappears or otherwise cleaves the DNA in to its constituents. Lane 6-10 represents SDS-CuNPs treated DNA with same increased concentrations as in CTAB-CuNPs. In lane 6 and 7 nicking of the DNA to form open circular (form II) and in the lane 8-10 a little bit formation of linear DNA (form III) were observed. For the same concentration the TEOS-CuNPs, lane 11-14, indicates that it strongly binds with the DNA and the open circular (form II) appears near the well and the mobility is found to be much slowed down. Lane 15-17 respectively represents the effect of SDS, TEOS and CTAB stabilized CuNPs at 20 μM with pUC18 DNA. It shows that at higher concentrations the anionic as well as the cationic CuNPs cleaves the DNA structure entirely, whereas the TEOS-CuNPs nick the DNA in to the open circular form (Form II) only.

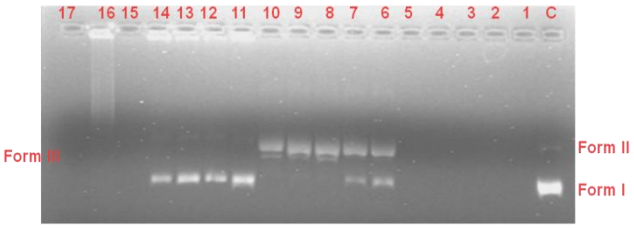

Figure 10. Agarose gel electrophoresis of pUC18 plasmid DNA with increasing concentrations of CuNPs. Incubation time 90 min at 37 ºC. lane C, supercoiled DNA pUC18; lane 1, DNA+5 μM CTAB-CuNPs; lane 2, DNA+7 μM CTAB-CuNPs; lane 3, DNA+10 μM CTAB-CuNPs; lane 4, DNA+12.5 μM CTAB-CuNPs; lane 5, DNA+16.5 μM CTAB-CuNPs; lane 6, DNA+5 μM SDS-CuNPs; lane 7, DNA+7 μM SDS-CuNPs; lane 8, DNA+10 μM SDS-CuNPs; lane 9, DNA+12.5 μM SDS-CuNPs; lane 10, DNA+16.5 μM SDS-CuNPs; lane 11, DNA+8 μM TEOS-CuNPs; lane 12, DNA+11 μM TEOS-CuNPs; lane 13, DNA+13 μM TEOS-CuNPs; lane 14, DNA+17 μM TEOS-CuNPs; lane 15, DNA+20 μM SDS-CuNPs; lane 16, DNA+20 μM TEOS-CuNPs and lane 17, DNA+20 μM CTAB-CuNPs.

3.3. 6. Structural morphology studies

In order to determine the morphology of the DNA in presence of cationic as well as anionic CuNPs, atomic force microscope was used with non-contact mode in solution. Figure 11a shows the image of pUC18 DNA with 1.3 μM cationic CuNPs. It reveals that in presence of cationic CuNPs the DNA forms spaghetti like (fishing net) and ellipsoidal frame work. The 2D and 3D images (Figure 11a) highlights the presence of brighter images of spherical CuNPs complexed with the circular DNA having reduced electrostatic repulsion to form different sizes of ellipsoids. The morphology of super coiled DNA with ~21 μM cationic CuNPs shows (Figure 12) the presence of linear and discrete chains with 2-4 μm in length, while the 2D and 3D images depicts that the CuNPs were attached to the base pairs to form a linear duplex structure and on increasing the CuNPs it reduce the electrostatic repulsion through complexation in the grooves [36]. It is evident that in the presence of cationic NPs the adjacent H-bonds in the DNA base are ruptured and hence the super coiled structure changes to linear one during the complexation. On the other hand the anionic NPs with super coiled DNA form spaghetti like (Figure 13a) embedded structure at lower concentrations and at higher concentrations it forms torroids like (Figure 13b) a ball on the palm structure. It shows that the thermodynamic constraints on such complexed DNA would favour mild distortion in the stiffness of polymeric units and the kinetic limits lead to the above structures (Figure 11, 12 and 13). The torsional strain induced by colloidal CuNPs at higher concentrations on the super coiled DNA gets readily relieved as the free ends twist to conformational changes along the entire length of DNA molecule. Then the DNA strands gets cleaved and complex with colloidal CuNPs and form microscopic images of ellipsoidal, torroidal and linear structures. This model is consistent with cooperative mechanisms of complexation/condensation in which the

super coiled DNA binds with charged colloidal CuNPs, reduce the folding strain at lower concentration to form a spaghetti/ellipsoidal like structures and at higher concentrations more relaxed linear and torroidal structures.

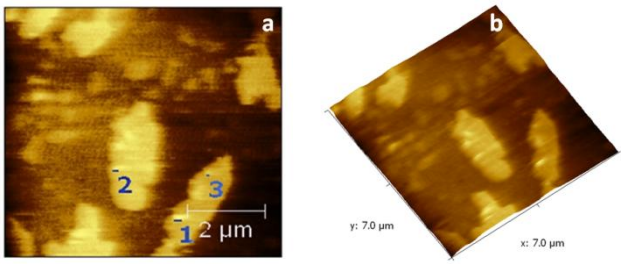

Figure 11. (a) 2D image of ellipsoidal structure of pUC18 with 1.3 µM CTAB-CuNPs and (b) its 3D image

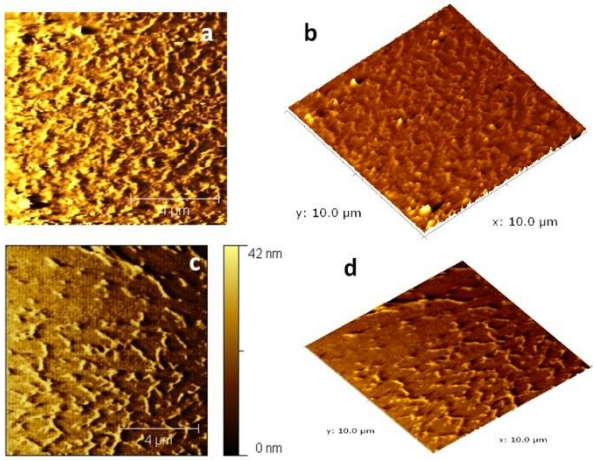

Figure 12. (a) AFM image of (2D) linear structure of pUC18 with 21 µM CTAB-CuNPs (b) its 3D image, (c) and (d) are fragmented linear structures of 2D and 3D images.

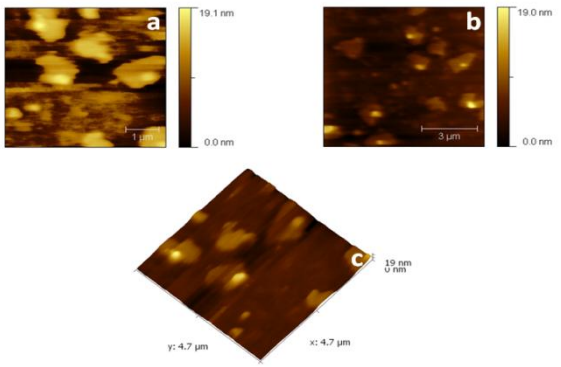

Figure 13. AFM image of (2D) linear structure of pUC18 with 21 uM cationically CuNPs (a) and (b),(c)3D image of b

The SEM and TEM images of CTAB capped CuNPs incubated with herring sperm DNA are given in figure 14. Interestingly, the dendrimer like clusters observed in the CTAB capped CuNPs is not observed after incubation with DNA, instead a chain like assembly is found with CuNPs imbedded on the major and minor grooves of the DNA through dipole-dipole interaction between the negatively charged phosphate backbone of the DNA and the positive dipole of the CuNPs.

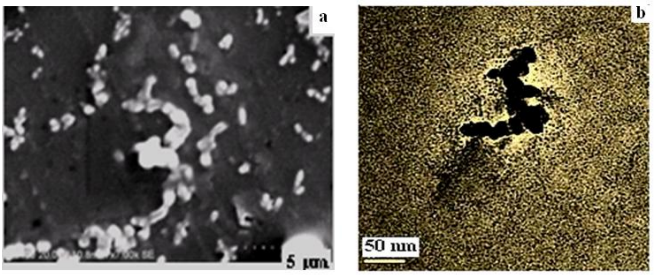

Figure 14. (a) SEM and (b) TEM images of CuNPs incubated with DNA

4 Conclusions

We have successfully synthesized long life copper nanoparticles, capped with anionic and cationic stabilizers, in aqueous solutions through reduction of cupric chloride by hydrazine hydrate under sonication. We believe that, the simultaneous use of citric acid and CTAB or SDS together with excess hydrazine is responsible for the observed higher stability (stable for more than 100 days). The differences in the binding of tetrapodal structured cationic cetyltrimethylammonium bromide stabilized copper nanoparticles and spherical shaped anionic sodium dodecyl sulphate stabilized copper nanoparticles with DNA is studied systematically and found that at lower concentrations form spaghetti/ellipsoid like structures with DNA, while at higher concentrations cleaves the DNA and form discrete chain-like assemblies. This may throw more light on the possibility of using CuNPs as drug carriers and in the development of nano-drug delivery systems, which are the subject matter of many scientists.

Acknowledgements

The financial support from the UGC-UPE, Madurai Kamaraj University and DST, New Delhi in the form of projects in Nanoscience & Nanotechnology are gratefully acknowledged. We thank Prof. C. Srinivasan, Emeritus Professor, Department of Materials Science for helpful discussions and Prof. S. Shanmugasundaram, School of Biological Sciences of our University for his help in AFM measurements and subsequent discussions. Further we thank the Central Instrumentation Facility, Pondicherry University for their help in recording SEM images.

References

[1] A. P. Alivisatos, *Science* 271 (1996) 933-937.
[2] J. Liu and Y. Bando, *Adv. Mater.* 15 (2003) 303-305.
[3] L. H. Reddy, J. L. Arias, J. Nicolas and P. Couvreur, *Chem. Rev.* 112 (2012) 5818-5878.
[4] A. Kamyshny and S. Magdassi in: T.F. Tadros (Ed.), *Colloid stability: the role of surface forces, part I, Nanoparticles in confined structures: formation and application*. Wiley-VCH, Weinheim (2006) pp. 207-234.
[5] D. V. Goia, *J. Mater. Chem.* 14 (2004) 451-458.
[6] R. C. Johnson, J. Li, J. T. Hupp and G. C. Scatz, *Chem. Phys. Lett.* 356 (2002) 534-540.

[7] C. Dolitis and W. L. Johnson *J. Appl. Phys.* 60 (1986) 1147-1151.
[8] L. Huang, E. S. Lee and K. B. Kim, *Colloids and Surfaces A physicochem. Eng. Aspects* 262 (2005) 125-131.
[9] X. Ren, D. Chen and F. Tang, *J. Phys Chem. B* 109 (2005) 15803-15807.
[10] M. P. Pileni, *J. Exp. Nanosci.* 1 (2006) 13-27.
[11] J. Wang, H. Huang, S. V. Kesapragada and D. Gall, *Nano Lett.* 5 (2005) 2505-2508.
[12] C. Wang, X. M. Zhang, X. F. Qian, Y. Xie, W. Z. Wang and Y. T. Qian, *Mater. Res. Bull.* 33 (1998) 1747-1751.
[13] H. H. Huang, F. Q. Yan, Y .M. Kek, C. H. Chew, G. Q. Xu, W. Ji, P. S. Oh and S. H. Tang, *Langmuir* 13 (1997) 172-175.
[14] S. H. Wu and D. H. Chen, *J. Colloid Interface Sci.* 273 (2004) 165-169.
[15] X. Zhang, H. Yin, X. Cheng, H. Hu, Q. Yu and A. Wang, *Mater. Res. Bull.* 41 (2006) 2041-2048.
[16] I. Lisiecki, F. Billoudet and M. P. Pileni, *J. Phys. Chem.* 100 (1996) 4160-4166.
[17] P. K. Khanna, S. Gaikwad, P. V. Adhyapak, N. Singh and R. Marimuthu, *Mater. Lett.* 61, (2007) 4711-4714.
[18] A. P. Alivisatos, K. P. Johnsson, X. Peng, T. E. Wilson, C. J. Loweth Jr and P. G. Schultz, *Nature* 382 (1996) 609-611.
[19] T. Torimoto, M. Yamashita, S. Kuwabata, T. Sakata, H. Mori and H. Yoneyama, *J. Phys. Chem. B* 103 (1999) 8799-8803.
[20] A. Kumar, M. Pattarkine, M. Bhadbhade, A. B. Mandale, K. N. Ganesh, S. S. Datar, C. V. Dharmadhikari and M. Sastry, *Adv. Mater.* 13 (2001) 341-344.
[21] C. F. Monson and A .T. Woolley, *Nano. Lett.* 3 (2003) 359-363.
[22] V. Sokolova and M. Epple, *Angew. Chem. Int. Ed.* 47 (2008) 1382-1395.
[23] J. Annaraj, S. Srinivasan, K. M. Ponvel and PR. Athappan, *J. Inorg. Biochem.* 99 (2005) 669-676.
[24] N. Prabakaran and PR. Athappan, *J. Inorg. Biochem.* 104 (2010) 712-717.
[25] Y. Kobayashi and T, Sakuraba, *Colloids and Surfaces A: Physicochem. Eng. Aspects* 317 (2008) 756-759.
[26] A. Wolf, G. H. Shimer and T. Meehan, *Biochemistry* 26 (1987) 6392-6396.
[27] Y. A. Lee, S. Lee, H. M. Lee and S. K. Kim, *J. Biochem.* 133 (2003) 343-349.
[28] A. Horn jr, I. Vencato, A. J. Bortoluzz, R. Horner, R. A. Nome Silva, B. Spoganicz, V. Drago, H. Terenzi, M. C. B. De Olivera, R. Werner, W. Haase and A. Neves, *Inorg. Chim. Acta* 358 (2005) 339-351.
[29] J. B. LePecq and C. Paoletti, *J. Mol. Biol.* 27 (1967) 87-106.
[30] S. Satyanarayana, J. C. Dabrowick and J. B. Chaires, *Biochemistry* 31, (1992) 9319-9324.
[31] Y. Xiang, X-F. He, X-H. Zou, J-Z. Wu, X-M. Chen, L-N. Ji, R. H. Li, J. Y. Zhou and K-B. Yu, *J.Chem. Soc. Dalton Trans.* (1999) 19-24
[32] V. I. Ivanov, L. E. Minchenkova, A. K. Schyolkina and A. I. Poletayev, *Biopolymers* 12, (1973) 89-110
[33] R. Ruiz, B. Garcia, J. G. Tojal, N. Busto, S. Ibeus, J. M. Leal, C. Martins, J. Gasper, J. Borras, R. Gil-Garcia and M. G. Alvarez, *J. Biol. Inorg. Chem.* 15 (2010) 525-532.
[34] M. Parkinson, M. Hawken, M. Hall, K. J. Sanders and A. Rodger, *Phys. Chem. Chem. Phys.* 2 (2000) 5469-5478.
[35] N. Kida, Y. Katsuda, Y. Yoshikawa, S. Komada, T. Sato, Y. Saito, M. Chikuma, M. Suzuki, T. Imanaka and K. Yoshikawa, *J. Biol. Inorg. Chem.* 15, (2010) 701-707.
[36] N.C. Seeman, *Nature* 421 (2003) 427-431.